Supporting Information

Selective Spectral Absorption of Nanofibers for Color-Preserving Daytime Radiative Cooling

Xiangshun Li [a], Huilin Xu [a], Yuchen Yang [a], Faxue Li, [a] Seeram Ramakrishna [b], Jianyong Yu [c], Dongxiao Ji [a,*], Xiaohong Qin [a,*]

[a]Key Laboratory of Textile Science & Technology, Ministry Education, College of Textiles, Donghua University, 2999 North Renmin Road, Songjiang, Shanghai, 201620, China.

[b]Department of Mechanical Engineering, National University of Singapore, Singapore 119260, Singapore.

[c]Innovation Center for Textile Science and Technology, Donghua University, Shanghai 201620, China.

Corresponding Authors:

E-mails: jidongxiao@hotmail.com (D. Ji),

E-mails: xhqin@dhu.edu.cn (X. Qin),

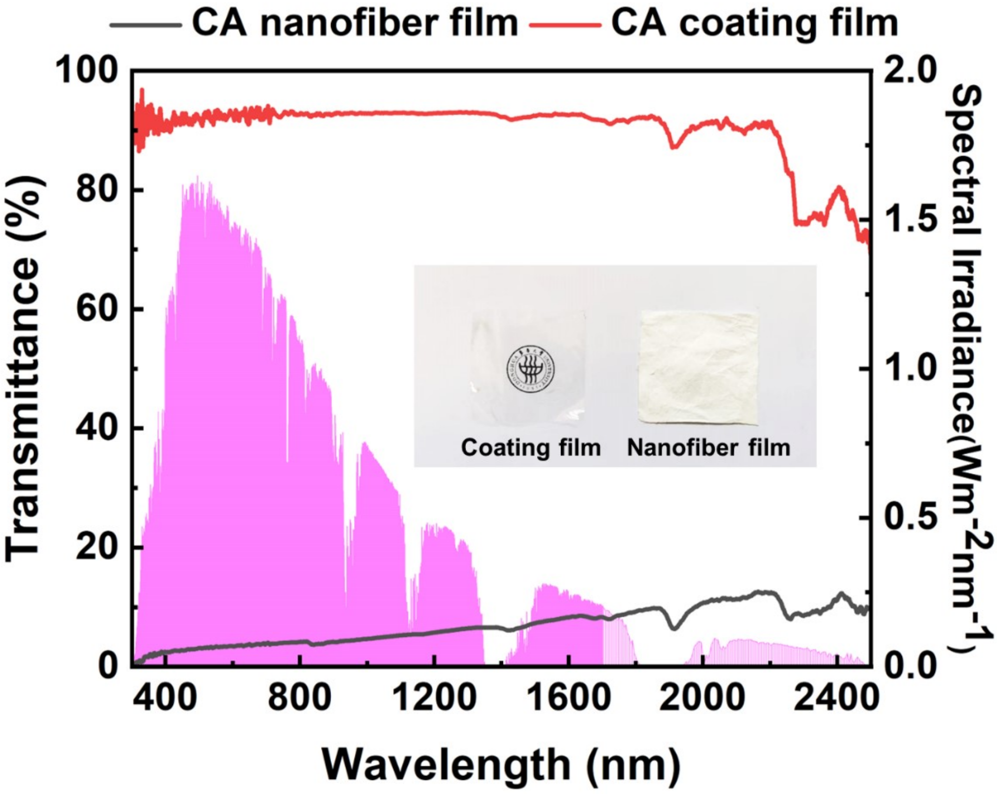

Fig. S1 Comparison of solar transmittance between CA nanofiber and CA film.

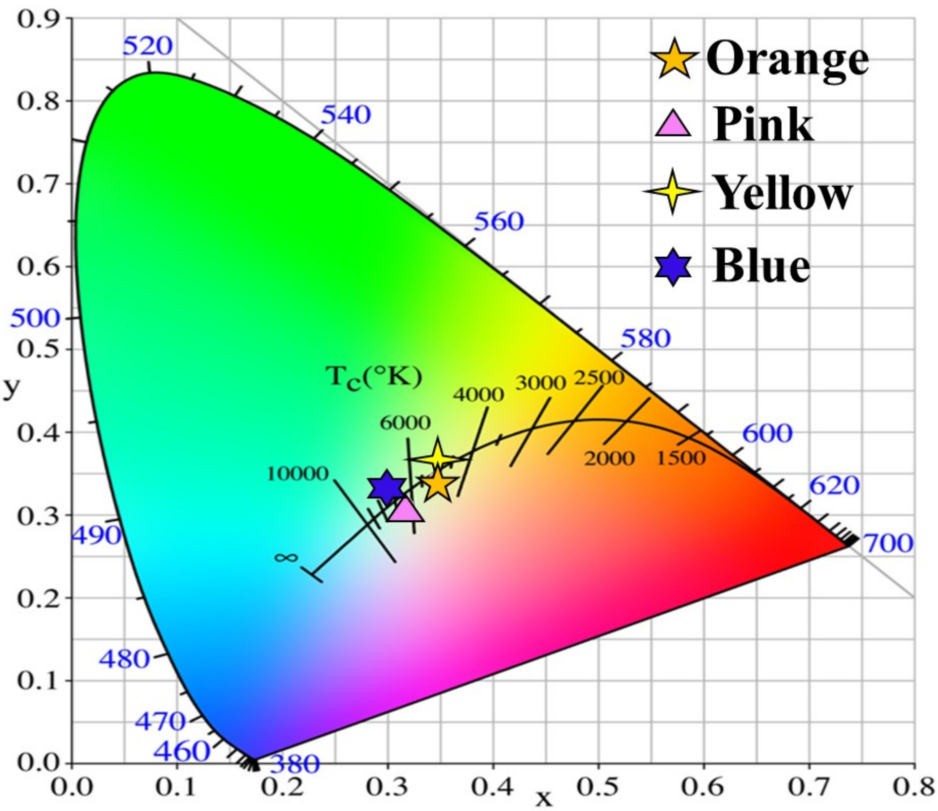

Fig. S2 The CIE chromaticity coordinates of the CA NF CSDRCs.

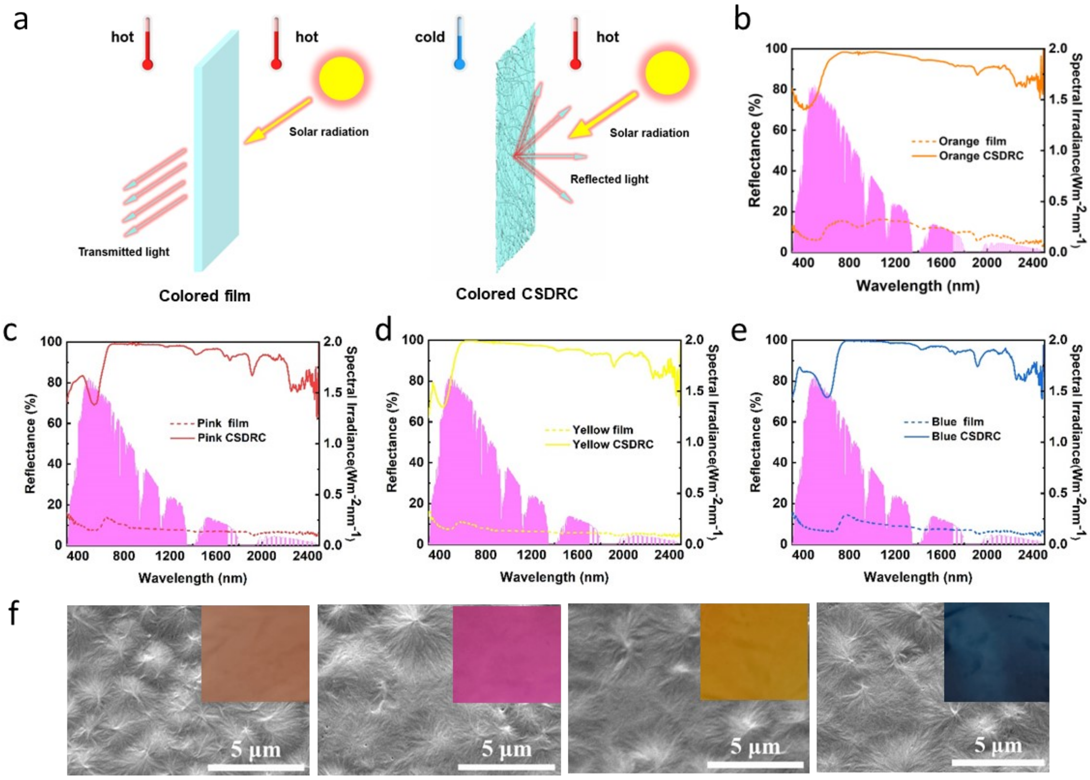

Fig. S3 (a) Schematic illustration of the solar radiation transmitted effect of CA NF CSDRC and CA film. (b ~ e) Comparison of solar reflectance between various colors CA NF CSDRCs and CA films. (f) SEM images of colored CA film, the photograph is embedded in the corresponding images.

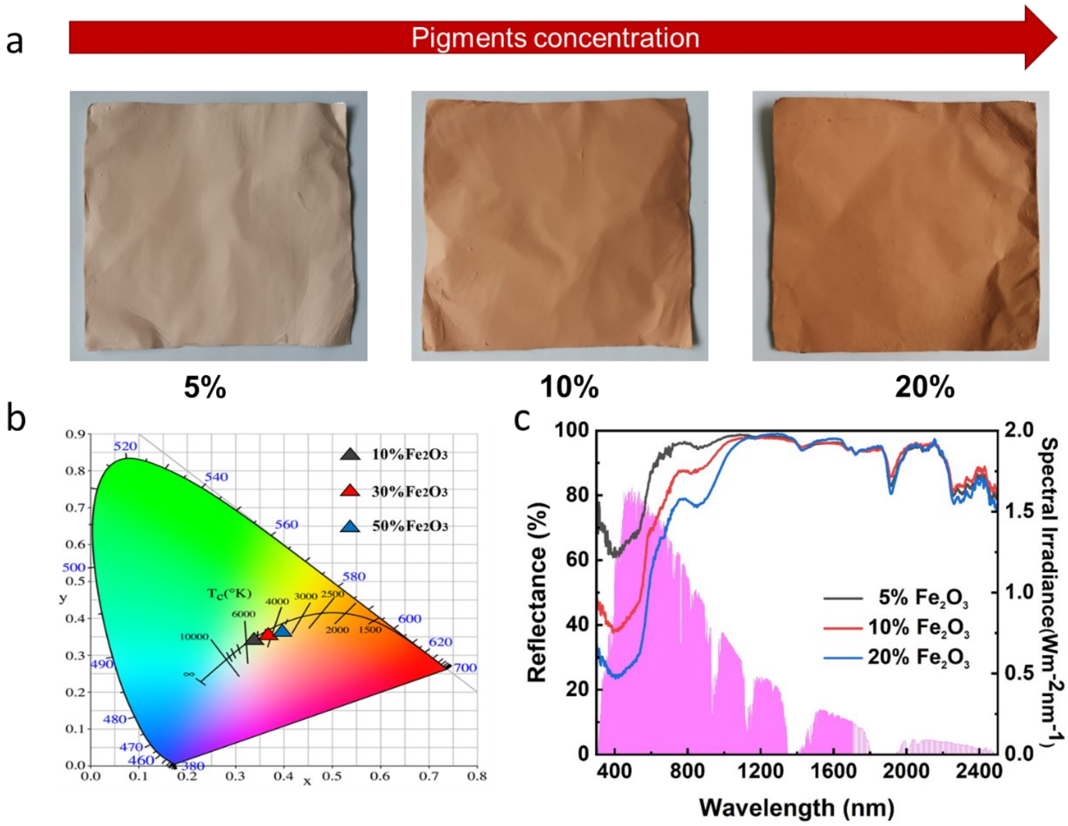

Fig. S4 (a) Photo images of orange CSDRC containing 5% ~ 20%Fe_2O_3. (b) The CIE chromaticity coordinates of the orange CSDRC with various concentrations of Fe_2O_3. (c) Reflectance spectra of orange CSDRC in the solar region.

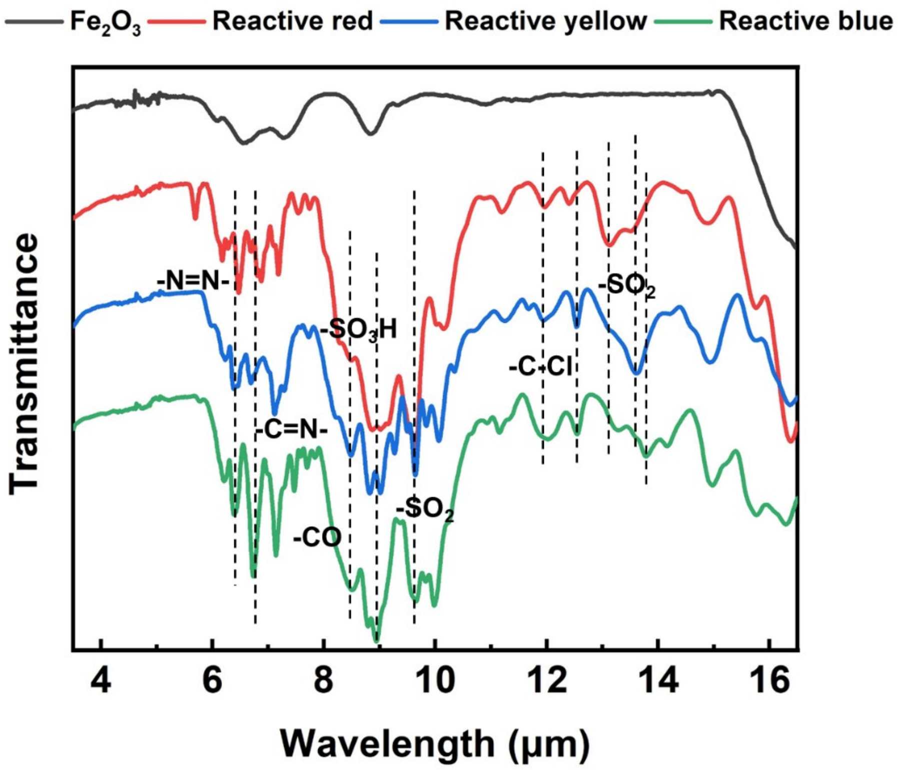

Fig. S5 IR spectrum of nano Fe_2O_3 pigment and reactive pink, yellow and blue dyes

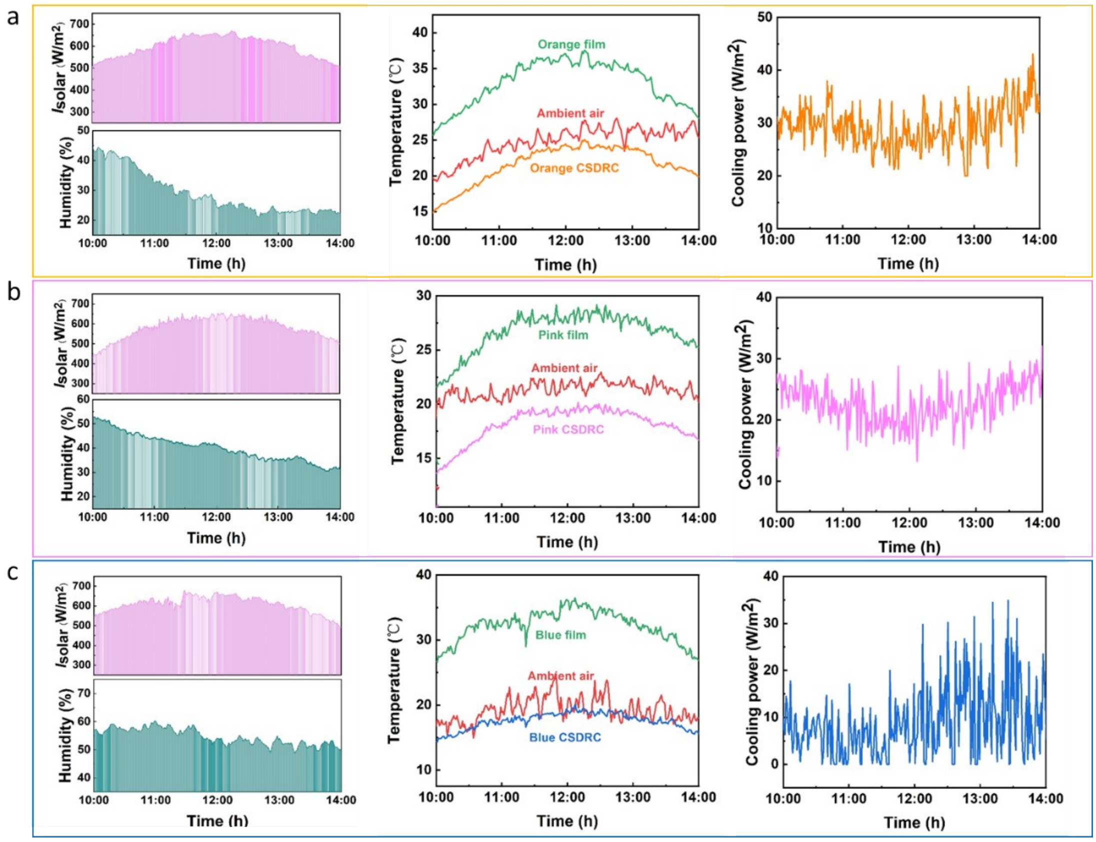

Fig. S6 Real-time monitoring temperature curve of (a) orange CSDRC, (b) pink CSDRC and (c) blue CSDRC in the outdoor test in Shanghai, China (Nov. 2022).

The comparison of cooling performance

We compared the cooling performance of CA NF CSDRC with recently reported colored daytime radiative coolers, founding that the daytime cooling capability of CA NF CSDRC is prominent due to the high NIR reflectance. Owing to no VIS absorption, the solar reflectance of the colored cooler in the Ref.7 is more than 95%, therefore the cooling effect is most obvious compared with other coolers. The Details of previous works are displayed in Table S3.

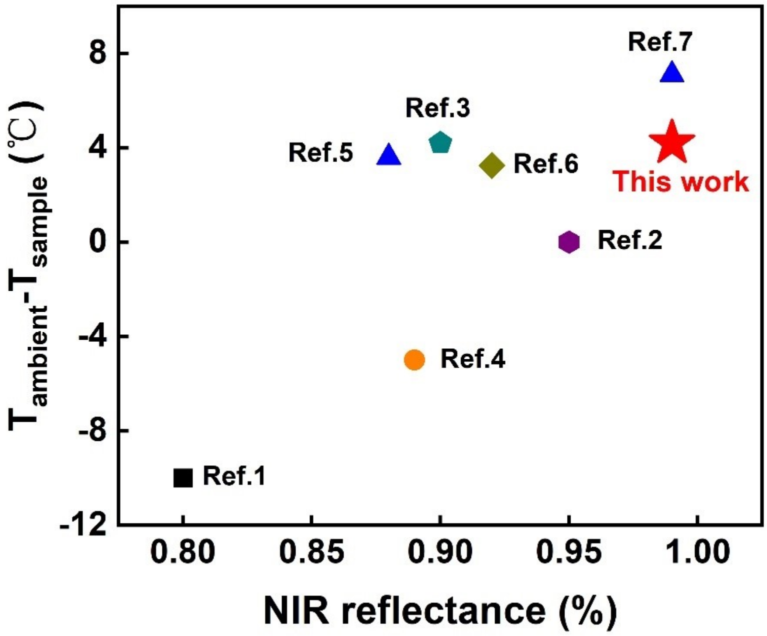

Fig. S7 Cooling temperature of recently reported colored daytime radiative coolers and the CA NF CSDRC in this work.

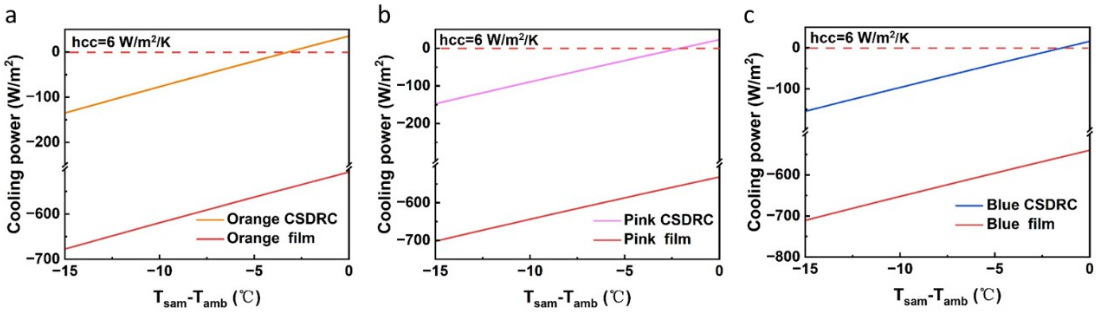

Fig. S8 The comparison of cooling power of (a) orange CSDRC, (b) pink CSDRC and (c) blue CSDRC and coating film (h_{cc} = 6 W/m^2/K).

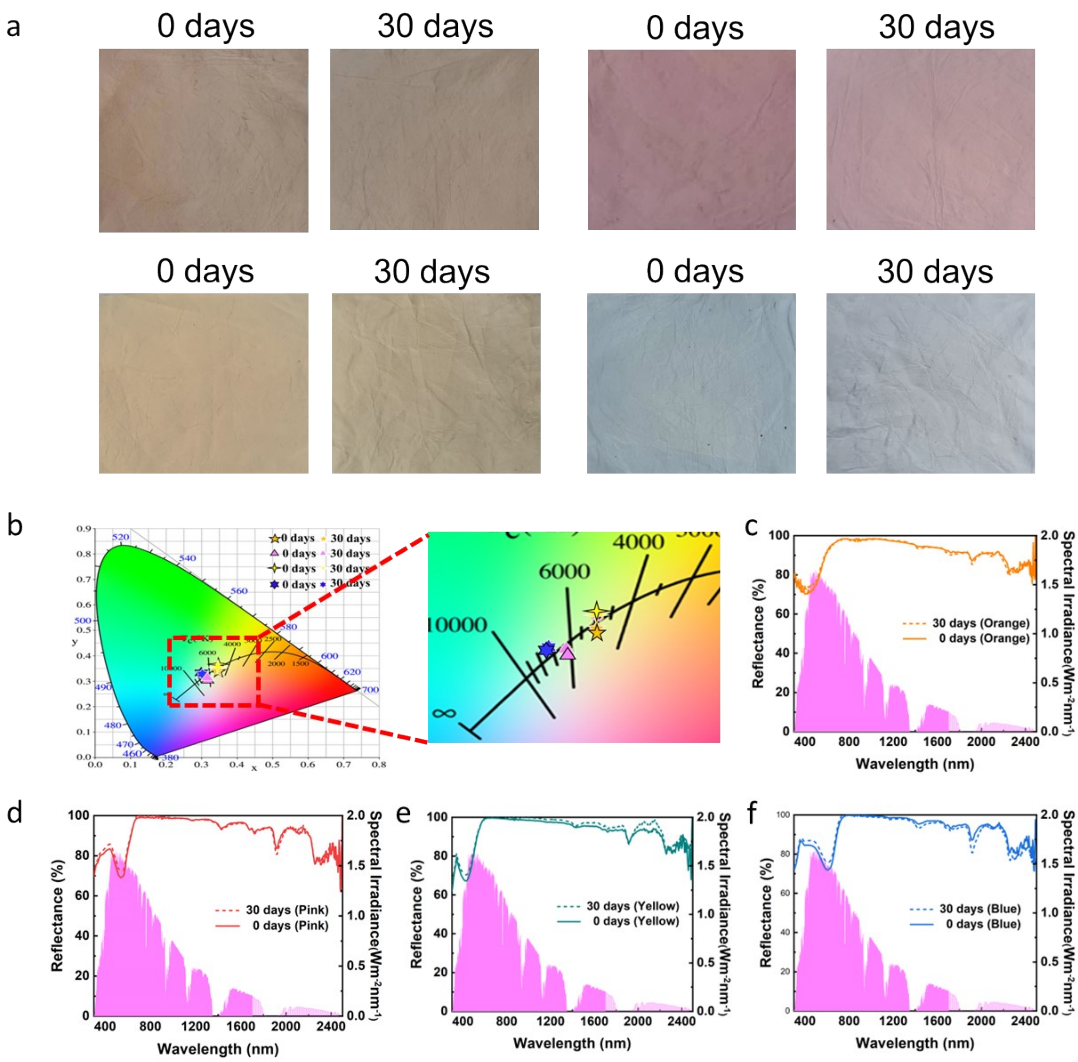

Fig. S9 (a) The photo picture and (b) the CIE chromaticity coordinates of CA NF CSDRC before and after 30 days of outdoor exposure. (c-f) The comparison of solar reflectance of the CA NF CSDRC before and after 30 days of outdoor exposure.

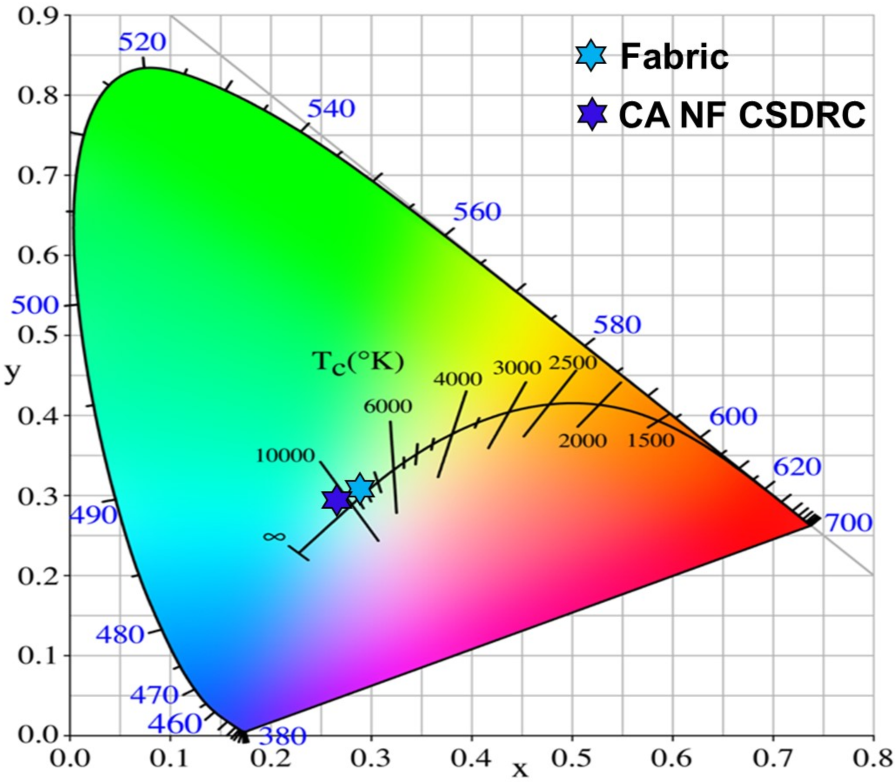

Fig. S10 The CIE chromaticity coordinates of CA NF CSDRC and fabric.

Table S1. Color properties of colorful nanofiber coolers

Samples	L	a*	b*
Orange CSDRC	90.20	7.65	9.82
Pink CSDRC	88.78	10.01	-5.03
Yellow CSDRC	93.79	1.14	18.72
Blue CSDRC	88.49	-2.09	-5.73

Table S2. The reflectivity values of the colored radiator in visible (0.4-0.8 μm; R_{VIS}) and near infrared wavelengths (0.8-2.5 μm; R_{NIR}), and the broadband solar reflectance (0.4-2.5 μm; R_{solar}), as well as the emittance in atmosphere windows (8-13 μm; ε_{AW}).

Sample / Optical property	Orange CSDRC	Pink CSDRC	Yellow CSDRC	Blue CSDRC
R_{VIS}	0.863	0.848	0.889	0.835
R_{NIR}	0.963	0.971	0.970	0.989
R_{Solar}	0.904	0.901	0.920	0.900
α_{Solar}	0.078	0.086	0.055	0.098
ε_{AW}	0.949	0.956	0.952	0.960

Table S3 A summary of information on the types of colored radiative coolers in recent years.

Ref.	Color	Structure	Materials	Method	Optical properties	Passive cooling performance (Power, Temperature and Solar radiation intensity)
1	Pink	Photonic structure color 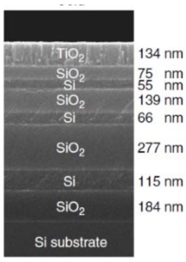	TiO_2, SiO_2, Si	1D stacks	Broadband ε_{ir}~0.8 R_{solar}~0.6 R_{NIR}~0.8	P_{sun}＞900 W/m^2 P:99.7W/m^2 ΔT: -10 °C
2	Cyan, magenta, and yellow	Photonic structure color 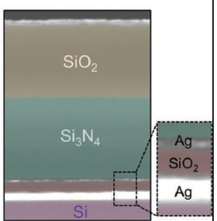	SiO_2, Si_3N_4, Ag, Si	1D stacks	Broadband ε_{ir}＞0.8 R_{NIR}＞0.9	P_{sun}＞900 W/m^2 ΔT: close to the air
3	Yellow, magenta, and cyan	Photonic structure color 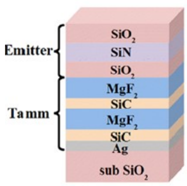	SiO_2, SiN, MgF_2, SiC, Ag	1D stacks	Broadband ε_{ir}~0.9 R_{NIR}~0.9	P_{sun}~800-900 W/m^2 P: 44.06 W/m^2 (yellow), 49.06 W/m^2 (magenta), 52.61 W/m^2 (cyan) ΔT_{yellow}: 4.2 °C $\Delta T_{magenta}$: 4.6 °C ΔT_{cyan}: 4.9 °C
4	black/blue/red/yellow	Bilayer colored paint 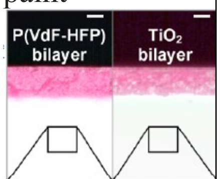	P(VdF-HFP), colorant	Coating	Broadband ε_{ir}＞0.95 R_{NIR}~0.89 R_{solar}:0.44 (black), 0.4 (blue), 0.61 (red), 0.72 (yellow)	P_{sun}~1000 W/m^2 ΔT_{black}:-25 °C, ΔT_{blue}:-22 °C, ΔT_{red}: -15 °C, ΔT_{yellow}: -5 °C

5	White, green and red	Four-layer film stack 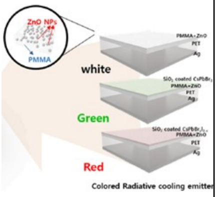	SiO_2-embedded perovskite NCs/PMMA+ZnO/PET/Ag	Deposition	Broadband $\varepsilon_{ir}\geq 0.95$ $R_{NIR} < 0.9$ R_{solar}:0.86 (white), 0.81 (green), 0.78 (red)	P_{sun}~900 W/m^2 ΔT_{white}: 4.2 °C ΔT_{green}: 3.6 °C ΔT_{red}: 1.7 °C
6	White, yellow, red, brown	Bilayer coating: Top-layer: QDs based color layer Bottom-layer: H-SiO_2/polymer nanoparticle white layer 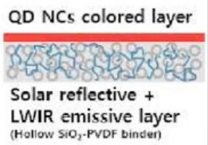	Cu-based quantum dots, H-SiO_2 /PVDF-HFP (the best), or PMMA, or PVP	Spay coating	Broadband ε_{ir}=0.943 $R_{NIR} > 0.9$ $R_{solar}\approx 0.97$ (white) ≈0.86 (yellow) ≈0.77 (red) ≈0.66 (brown)	P_{sun}~800 W/m^2 ΔT_{white}: 6.12 °C ΔT_{yellow}: 3.25 °C ΔT_{red}: 0.51 °C ΔT_{brown}: -3.24 °C
7	Indigo, blue, green, yellow, and pink	Photonic structure color 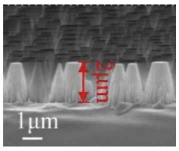	SiO_2	self-assembly method and reactive ion etching	Broadband ε_{ir}=0.95 $R_{NIR} > 0.9$ $R_{solar} > 0.95$	P: 143 W/m^2 ΔT: 7.1 °C

Table S4 Weather Forecast in Shanghai in Nov. 2022

Date	T_{max} (°C)	T_{min} (°C)	Weather	Wind Power
2022-11-01	20	15	Cloudy to overcast	Breeze
2022-11-02	20	14	Sunny	Breeze
2022-11-03	21	15	Cloudy	Breeze
2022-11-04	18	12	Cloudy to overcast	Breeze
2022-11-05	18	12	Cloudy to sunny	Breeze
2022-11-06	19	13	Sunny	Breeze
2022-11-07	22	14	Sunny	Breeze
2022-11-08	22	16	Sunny to cloudy	Breeze
2022-11-09	23	17	Cloudy to sunny	Grade 3-4
2022-11-10	23	17	Cloudy to overcast	Breeze
2022-11-11	23	19	Light rain	Grade 3-4
2022-11-12	26	16	Cloudy to light rain	Grade 3-4
2022-11-13	17	12	Overcast to Sunny	Breeze
2022-11-14	13	10	Cloudy to overcast	Breeze
2022-11-15	17	10	Overcast	Breeze
2022-11-16	17	13	Overcast to light rain	Grade 3-4
2022-11-17	17	15	Light rain turns overcast	Breeze
2022-11-18	20	16	Light rain	Breeze
2022-11-19	19	16	Light rain	Breeze
2022-11-20	19	15	Cloudy to sunny	Breeze
2022-11-21	20	15	Cloudy to light rain	Breeze
2022-11-22	19	13	Light rain to cloudy	Breeze
2022-11-23	18	13	Cloudy to sunny	Breeze
2022-11-24	17	14	Cloudy	Breeze
2022-11-25	20	13	Cloudy to light rain	Breeze
2022-11-26	19	16	Cloudy to overcast	Grade 3-4
2022-11-27	21	18	Light rain to overcast	Breeze
2022-11-28	21	16	Moderate rain to light rain	Grade 4-5
2022-11-29	17	5	Light rain	Grade 5-6
2022-11-30	6	3	Light rain	Breeze

Supplementary Note 1：Calculation of radiative cooling power

The net cooling power (P_{net}) of the colored flexible nanofiber cooler can be calculated as follows [8-11]:

$$P_{net} = P_{rad} - P_{atm} - P_{solar} - P_{cond+conv}$$

where P_{rad} is the energy radiated into space, P_{atm} is the atmospheric radiative energy absorbed, P_{solar} is the solar energy absorbed, and $P_{\text{cond+conv}}$ represents the non-radiative parasitic losses.

$$P_{rad} = \pi \int_0^{+\infty} \int_0^{\frac{\pi}{2}} \varepsilon_r(\lambda,\theta) I_b(\lambda, T_{sur}) \sin(2\theta) d\theta d\lambda$$

where $\varepsilon_r(\lambda,\theta)$ is the spectral emissivity. Here, T_{sur} represents the surface temperature. $I_b(\lambda,T_{sur})\cos(\theta)$ represents the intensity of black-body radiations at T_{sur}, which is taken as: $I_b(\lambda, T_{sur}) = \frac{2hc^2}{\lambda^5} \frac{1}{e^{\frac{hc}{\lambda KT}} - 1}$, where h, c and k are Planck's constant, speed of light in vacuum and Boltzmann's constant, respectively.

$$P_{atm} = \pi \int_0^{+\infty} \int_0^{\frac{\pi}{2}} \alpha_r(\lambda,\theta) \varepsilon_{atm}(\lambda,\theta) I_b(\lambda, T_a) \sin(2\theta) d\theta d\lambda$$

Where $\alpha_r(\lambda,\theta)$ refers to the spectral absorptivity of the cooler and equals to the spectral directional emissivity $\varepsilon_r(\lambda,\theta)$ based on Kirchhoff's law of thermal radiation. T_a is the ambient temperature. where $\varepsilon_{atm}(\lambda,\theta)$ is the spectral directional emissivity of the sky atmosphere, which can be expressed as:

$$\varepsilon_{atm}(\lambda,\theta) = 1 - [\tau(\lambda,\theta)]^{1/\cos(\theta)}$$

where (λ,θ) represents the atmospheric transmissivity at vertical direction.

$$P_{sun} = \int_0^{+\infty} I_{AM1.5}(\lambda) \alpha_r(\lambda, \theta_{sun}) d\lambda$$

where $I_{AM1.5}(\lambda)$ is the AM 1.5 spectrum distribution of the solar radiation intensity varying with the wavelength.

$$P_{cond+conv} = h_{cc}(T_a - T_{sur})$$

$P_{cond+conv}$ is the power density of nonradiative heat exchange due to convection and conduction. The h_{cc} is a comprehensive heat transfer coefficient. It is closely related to the local wind speed. The dependence of h on the local wind speed can be qualitatively modeled using a simple empirical expression

$$h_{cc}=2.5+2V_{wind}$$

where V_{wind} represents the wind speed expressed in m/s. We set h_{cc} values as 0 W/m^2, 3 W/m^2, 6 W/m^2, and 12 W/m^2, respectively, to show the impact of different non-radiative heat exchange coefficient on affecting the cooling performance. During Nov. 2022, the average wind speed in Shanghai was around 3-5 m/s (Table S4), suggesting likely h_{cc} values in the range around 6-12 W/m^2.

References

1. W. Li, Y. Shi, Z. Chen and S. Fan, *Nat Commun*, 2018, **9**, 4240.

2. G. J. Lee, Y. J. Kim, H. M. Kim, Y. J. Yoo and Y. M. Song, *Advanced Optical Materials*, 2018, **6**, 1800707.

3. C. Sheng, Y. An, J. Du and X. Li, *ACS Photonics*, 2019, **6**, 2545-2552.

4. J. M. Yijun Chen, Wenxi Li, Ajani Smith-Washington, Cheng-Chia Tsai,Wenlong Huang, Sajan Shrestha, Nanfang Yu, Ray P. S. Han, Anyuan Cao, Yuan Yang, *science advances*, 2020, **6**, eaaz5413.

5. S. Son, S. Jeon, D. Chae, S. Y. Lee, Y. Liu, H. Lim, S. J. Oh and H. Lee, *Nano Energy*, 2021, **79**, 105461.

6. T. Y. Yoon, S. Son, S. Min, D. Chae, H. Y. Woo, J.-Y. Chae, H. Lim, J. Shin, T. Paik and H. Lee, *Materials Today Physics*, 2021, **21**, 100510.

7. Z. Ding, L. Pattelli, H. Xu, W. Sun, X. Li, L. Pan, J. Zhao, C. Wang, X. Zhang, Y. Song, J. Qiu, Y. Li and R. Yang, *Small*, 2022, **18**, e2202400.

8. T. Wang, Y. Wu, L. Shi, X. Hu, M. Chen and L. Wu, *Nat Commun*, 2021, **12**, 365.

9. H. H. Kim, E. Im and S. Lee, *Langmuir : the ACS journal of surfaces and colloids*, 2020, **36**, 6589-6596.

10. A. P. Raman, M. A. Anoma, L. Zhu, E. Rephaeli and S. Fan, *Nature*, 2014, **515**, 540-544.

11. S. Fan and W. Li, *Nature Photonics*, 2022, **16**, 182-190.